Front. Electr. Electron. Eng. China 2010, 5(2): 119–127
DOI 10.1007/s11460-010-0012-3

RESEARCH ARTICLE

Zhijun CAI, Ge WANG, Er-Wei BAI

Adaptive bolus chasing computed tomography angiography by a local linear time and space parameter varying model: modeling, control, identification, and experimental results

Abstract A high contrast to noise ratio (CNR) is always desirable for contrast-enhanced computed tomography angiography (CTA). To ensure a high CNR of the vascular images in CTA and potentially reduce the radiation exposure and contrast usage, an adaptive bolus chasing method is proposed and evaluated compared to the existing constant-speed method. The proposed method is based on a local time and space parameter varying model of the contrast bolus. Optimal scan time for the next segment of the vasculature is estimated and predicted in real time and guides the computed tomography (CT) scanner table movement that guarantees that each segment of the vasculature is scanned with the maximum possible enhancement. Simulations and experimental results show that the proposed bolus chasing method outperforms the conventional constant-speed method substantially.

Keywords adaptive control, bolus chasing computed tomography angiography (CTA), local linear time and space parameter varying model

1 Introduction

Today, computed tomography angiography (CTA) has become more and more important in evaluating vascular diseases due to its accurate, fast, and noninvasive characteristics [1–3]. To obtain a better quality diagnosis image, a contrast medium (bolus) is injected into a vein before performing a computed tomography (CT) scan. The contrast bolus flows along with the blood in the human circulatory system. It is highly desirable that every segment of the artery be scanned at the time when the contrast bolus peak arrives, which maximally enhances the signal to background noise ratio. To this end, the synchronization of the X-ray aperture of the CT scanner and the contrast bolus peak is crucial to the diagnosis image quality.

It has been long realized that the current technology that transports a CT table in a prescribed constant movement is problematic due to the highly nonlinear dynamics of the contrast bolus [4–6]. The contrast bolus can be affected by many factors, such as heart function, contrast injection method, and vasculature diseases. The constant-speed method is simply incapable of synchronizing the contrast bolus peak and the X-ray aperture. A compensation for this is to increase the dosage of the contrast medium so that the contrast concentration is high for a long distance in the artery, and the chance to miss the bolus is reduced. However, this does not solve the problem completely, because 1) the contrast medium is harmful, especially for patients with kidney diseases, and 2) the choice of the preset speed is unclear, which could result in under or over-chasing, as reported extensively in Refs. [1,6].

To that end, an adaptive bolus chasing method, which guarantees a higher contrast to noise ratio (CNR), is imperative. The bolus chasing method is not a very new concept in the angiograms. It has been studied in digital subtraction angiography (DSA) [7] and magnetic resonance angiography (MRA) [8–12]. However, both DSA and MRA modalities have a larger field of view (FOV) in the z direction. The contrast bolus peak most likely stays inside the FOV for MRA and DSA, and positioning the table several times accordingly is good enough to chase the contrast bolus. However, a typical four-detector row CT scanner (Siemens Somatom Volume Zoom) has a

Received January 21, 2010; accepted February 24, 2010

Zhijun CAI, Er-Wei BAI (✉)
Department of Electrical and Computer Engineering, University of Iowa, Iowa City, IA 52242, USA
E-mail: er-wei-bai@uiowa.edu

Ge WANG
VT-WFU School of Biomedical Engineering & Sciences, Virginia Polytechnic Institute & State University, Blacksburg, VA 24061, USA

maximum FOV of 2 cm in z direction, which provides little information of the bolus peak and velocity. To overcome this, the contrast bolus dynamics should be studied carefully, and an effective and robust real-time estimation method needs to be proposed.

In our previous works, we have collected and investigated hundreds of clinical MRA and DSA datasets. The contrast bolus dynamics were carefully analyzed and applied in the adaptive optimal controller design [13], where a bivariate second-order polynomial is used to approximate the bolus density function. Though the tracking results are good and the proposed chasing method outperforms the current constant velocity method substantially, local linear modeling based on the contrast bolus information should bring additional benefits.

Modeling contrast bolus dynamics is challenging not only because of the complication of the circulatory system but also the interaction of the contrast medium and the blood dynamics. Contrast bolus flows along the vasculature. Its dynamics are related to the human blood and its concentration attenuates due to dispersion. There are a number of models that have been proposed for the contrast bolus. The gamma model [14] and the lagged normal density model [15] only describe the bolus temporal curve at some fixed positions, while no information about the bolus spatial profile is given, which is critical in bolus chasing. A nearly complete bolus model is built through a set of differential equations in Ref. [16]. However, it needs too many unknown parameters, which prevents its use in real-time application.

In this paper, we will first derive the contrast bolus dynamics from the diffusion-convention equation and then propose an optimal adaptive controller to chase the contrast bolus peak. Finally, we will provide simulation and experimental results to show that the proposed controller is able to chase the contrast bolus peak well and outperform the constant-speed method substantially.

2 Contrast bolus model

2.1 Derivations

As mentioned before, the reported bolus models are either simple but lack spatial information or adequate but too complicated. For the purpose of the adaptive bolus chasing techniques, we need a simple model containing bolus spatial profile that can be implemented in real time, and at the same time, the model has to be versatile enough that it is applicable to patients with various disease conditions. In Ref. [17], a bolus model, which is a function of time and distance, is derived from the one-dimensional convective function. Based on this diffusion-convection equation [17], our model is further developed in the form of a local linear time and space parameter varying model for the adaptive bolus chasing purpose.

In Fig. 1, the blood vessel wall is denoted by the thick lines. Let $C(z,t)$ denote the bolus concentration at distance z and time t and $A(z)$ denote the cross section area. Q is the flow rate for the whole segment. Within a small segment, we assume that the cross sectional area is a constant, i.e.,

$$A(z-\mathrm{d}z) = A(z) = A.$$

According to the continuity law, the mass change from time t to $t+\delta t$ in the small segment is

$$[C(z,t+\delta t) - C(z,t)]A\mathrm{d}z. \tag{1}$$

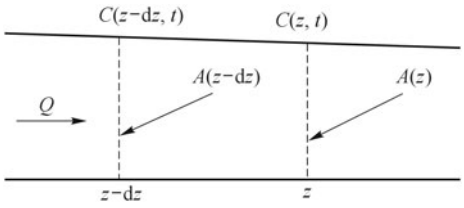

Fig. 1 Schematic of a segment of blood vessel

On the other hand, the mass flow into the small segment at $z-\mathrm{d}z$ is composed of 1) flow-induced $C(z-\mathrm{d}z,t)Q\delta t$ and 2) density-gradient-induced $-K\left.\frac{\partial C}{\partial z}\right|_{z-\mathrm{d}z}$ (under the assumption that the flow is proportional to density gradient, and K is the diffusion coefficient). The same situation applies to the mass flowing out the small segment. By mass conservation law, the mass change must equal the mass difference between flow coming in and the flow going out:

$$\begin{aligned}&[C(z,t+\delta t) - C(z,t)]A\mathrm{d}z\\ &= [C(z-\mathrm{d}z,t) - C(z,t)]Q\delta t\\ &\quad + \left(-K\left.\frac{\partial C}{\partial z}\right|_{z-\mathrm{d}z} + K\left.\frac{\partial C}{\partial z}\right|_{z}\right)\delta t.\end{aligned} \tag{2}$$

By expanding $C(z-\mathrm{d}z,t)$ and neglecting the higher order terms, we have

$$\frac{\partial C(z,t)}{\partial t} + v\frac{\partial C(z,t)}{\partial z} - \mu\frac{\partial^2 C}{\partial z^2} = 0, \tag{3}$$

where

$$v = \frac{Q}{A}$$

and

$$\mu = \frac{2K + Q\mathrm{d}z}{2A},$$

which is a standard convection diffusion equation. It is different from that of Ref. [17] due to the diffusion effect.

The solution of Eq. (3) depends on the boundary condition. Assuming we have an impulse input $\delta(t)$ at $z=0$ and $t=0$ with magnitude M. Using the same technique described in Ref. [17], we have the solution:

$$C(z,t)=\frac{M}{\sqrt{4\pi\mu t}}\mathrm{e}^{-\frac{(z-vt)^2}{4\mu t}}. \tag{4}$$

Unfortunately, this solution is not ready to be implemented in the controller because:

1) The cross-sectional area of the blood vessel remains constant only in a small segment.

2) The flow rate is varying due to the vascular branches.

3) The boundary condition is not practical.

However, this solution provides us some information about the contrast bolus. First, at any distance, the bolus temporal profile is bell-shaped, and second, the magnitude of the contrast peak concentration attenuates as time goes on.

2.2 Fitting results

Before applying Eq. (4) to the controller design, we verify the model by clinical MRA data collected from University of Iowa Hospital and Clinics (UIHC) and Northwestern University (NU) (see Ref. [18] for details). The reason to use MRA datasets is twofold:

1) As we mentioned before, CT has a small FOV in the z direction, and therefore, it is nearly impossible to record the contrast dynamics for a long distance (z direction) during a long time (from the beginning to the end). Hence, we have to use the bolus data recorded other than CTA.

2) DSA and MRA are the other two image modalities that are capable of scanning a large FOV with high-quality image sequences. With these two imaging modalities, MRA has the advantage of having the similar contrast bolus injection site (vein) and method, which means that the bolus dynamics would be similar to that of the CTA. Each collected MRA image sequence contains 30 images of the aorta at a rate of one image per second. The bolus arrival time varies from 10 to 25 seconds. The bolus concentration level is approximately proportional to the signal intensity obtained from MRA images.

We first use model (4) to fit the bolus temporal profile at each distance along the aorta and then put those temporal curves into a three-dimensional (3D) profile. Figure 2 shows the typical bolus temporal profile and fitting results, while Fig. 3 gives the actual and fitted 3D bolus profile. It can be concluded that the bolus temporal profile is well fitted in Figs. 2 and 3. However, model (4) does not show the ability to fit the 3D bolus profile for a long distance. The reason is twofold:

1) The boundary condition is just an assumption, and it never happens in reality.

2) When we fit the bolus in a longer distance, the vasculature curvature and branches should be considered.

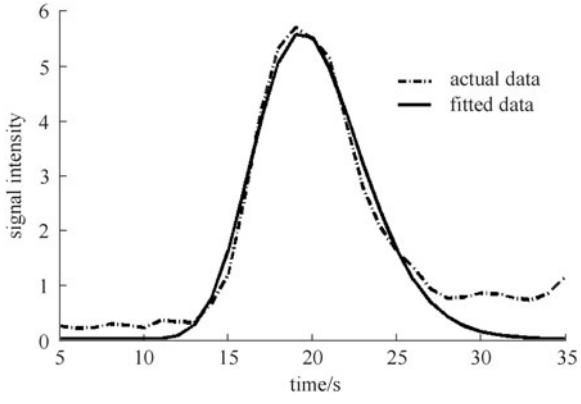

Fig. 2 Bolus temporal profile

2.3 Linear time and space parameter varying model

The main objective of bolus chasing CTA is to scan the vasculature with the highest possible concentration of

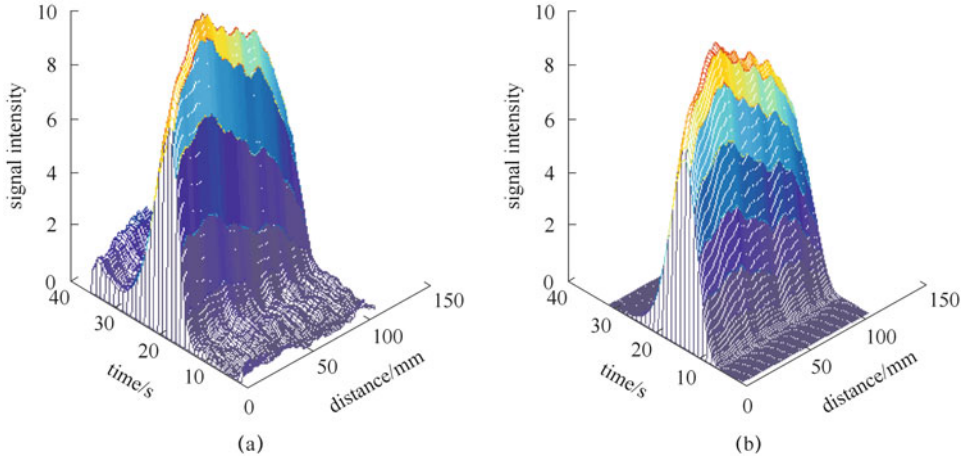

Fig. 3 3D Bolus profile. (a) Actual 3D bolus profile; (b) fitted 3D bolus profile

contrast so that the vasculature is optimally enhanced. To that end, we need a model that can predict the bolus peak position in real time locally regardless of the patient weight, heart function, and injection method. The aforementioned partial differential equation (PDE) model is a good candidate but is not suggested to be used directly in the controller design due to its nonlinear property. Identification of unknown parameters in the model is a nonlinear problem, and the local optimum versus global minimum is always a tricky issue. However, this PDE model does provide us a base for deriving a local model. Observe that the vasculature is scanned segment by segment, and the purpose of a local model is to provide enough information for a particular segment. To that end, we transform the PDE model into a local linear time and space parameter varying (LPV) model under the condition. First, the exponential function is expanded in the neighborhood of $z = vt$, around where the contrast has the highest concentration.

$$C(z,t) = \frac{M}{\sqrt{t}}\left[1-\frac{(z-vt)^2}{4\mu t}\right] = \frac{M}{\sqrt{t}}\left(1-\frac{z^2-2zvt+v^2t^2}{4\mu t}\right). \quad (5)$$

Now, the bolus model can be represented by a polynomial:

$$C(z,t) = a_1 t^{-\frac{1}{2}} + a_2 t^{\frac{1}{2}} + a_3 z t^{-\frac{1}{2}} + a_4 z^2 t^{-\frac{3}{2}}, \quad (6)$$

where $a_1 = M$, $a_2 = -\frac{Mv^2}{4\mu}$, $a_3 = \frac{Mv}{2\mu}$, and $a_4 = -\frac{M}{4\mu}$.

Remark 1) The choice of a local model is not unique. Eq. (5) is probably the most convenient and straightforward.

2) Although related, those four parameters are treated independently in modeling for simplicity and also for the increased degree of freedom that translates into an improved fitting ability. While we can add higher order terms to improve the accuracy, it will increase the number of parameters, and the results are not necessarily improved.

3) The local linear time and space parameter varying model here contains only four unknown parameters as compared to the six in our previous works [13]. This model is simpler because it is based on the actual bolus dynamic equation.

Since Eq. (6) is a local model of the contrast bolus, the coefficients are, in fact, time and space dependent or varying:

$$C(z,t) = a_1(z,t)t^{-\frac{1}{2}} + a_2(z,t)t^{\frac{1}{2}} + a_3(z,t)zt^{-\frac{1}{2}} + a_4(z,t)z^2t^{-\frac{3}{2}}. \quad (7)$$

3 Problem formulation and control algorithm design

3.1 Problem formulation

Before designing the tracking algorithm, we need to formulate the problem carefully. Generally, we want to continuously track the contrast bolus peak position while the contrast bolus flows along the vasculature. This is true when there is only one peak in the whole vasculature and the peak flows from the aorta to the arteries in the foot. However, that situation rarely happens due to the length of time involved in the injection and vascular diseases. For instance, the contrast bolus peak is likely to stay in an aneurysm for a longer time. On the other hand, what physicians need are the well-enhanced images for every segment of the vasculature. Therefore, the bolus chasing CTA problem can be stated as follows:

Design an adaptive control algorithm to transport the CT table so that each segment of the vasculature is optimally enhanced. The control algorithm should be robust to patient weight, heart function, and vasculature diseases and injection methods.

3.2 Control algorithm design

Mathematically, if the contrast bolus density function $C(z,t)$ is available, the control objective is to find a function $t(z)$ that maximizes the average bolus density over the scan length,

$$t^*(z) = \arg\max_{t(z)} \int_0^{z_e} C(z,t(z))\mathrm{d}z, \quad (8)$$

where z_e is the scan length.

Due to the inherent discrete-time nature of a CT scanner, it is more appropriate to use discrete time formulation. To this end, we segment the scan range z_e into N sections, and let $z_k = kz_e/N$, $k = 0,1,2,...,N$. Therefore, the control objective turns into finding a time sequence $t_k(z_k)$ that solves the following minimization:

$$\{t^*(z_k)\}_{k=0}^N = \arg\max_{\{t(z_k)\}_{k=0}^N} \sum_{i=0}^N C(z_i,t(z_i)). \quad (9)$$

Since the actual bolus information $C(z,t)$ is unknown and only its local estimate $\{\hat{C}_k(z_{k+1},t)\}_{k=0}^{N-1}$ is available, the control objective becomes at position z_k, to find

$$\bar{t}(z_k) = \arg\max_{t(z_k)} \hat{C}_{k-1}(z_k,t(z_k)),\ k = 1,2,...,N, \quad (10)$$

which gives rise to the maximum bolus density at z_{k+1}. In reality, the table velocity is also under the constraints of patient comfort level

$$0 < \frac{z_e/N}{\Delta_b} \leqslant \frac{\mathrm{d}z}{\mathrm{d}t} \leqslant \frac{z_e/N}{\Delta_s} < \infty$$

for some Δ_b and $\Delta_s > 0$. The first inequality indicates that the CT table can only move forward, and the second one imposes on the maximum velocity on the table. Under these constraints, the control algorithm is modified as

$$\bar{t}_k = \begin{cases} \bar{t}_{k-1} + \Delta_s, & \text{if } \bar{t}_k(z_k) \leqslant \bar{t}_{k-1} + \Delta_s, \\ \bar{t}_{k-1} + \Delta_b, & \text{if } \bar{t}_k(z_k) \geqslant \bar{t}_{k-1} + \Delta_b, \\ \bar{t}_k(z_k), & \text{otherwise.} \end{cases} \tag{11}$$

It can be shown in a similar way, as in Ref. [13], that the above control scheme is robust in the sense that a small estimation error between the estimate $\hat{C}(z,t)$ and the actual $C(z,t)$ would result in a small tracking error.

3.3 Estimation

In the above control algorithm, the critical part is to identify the approximation function $\hat{C}_k(z_k,t)$ in the form of Eq. (7) and find the optimal time sequence $\bar{t}_k$ in real time. Before the identification procedure is presented, some features of the CT scanner should be stated:

1) In present day, multidetector row CT scanners are very common, and it is reasonable to assume that the CT scanner has rows of detectors. Thus, at a given time t_k, we are able to observe the bolus density at the current position z_k as well as at $z_k + \delta_z$, where δ_z is decided by the scanner. In this paper, we let $\delta_z = 2.5$ mm [19].

2) CT gantry rotation speed is set to $\Delta T = 1/3$ second per rotation, a standard in modern CT practice.

3) CT image reconstruction time is negligible considering that the real CT scanner has a very fast computer and just a low resolution is needed during the tracking procedure.

4) The maximum patient table speed in a modern CT is about 10 cm/s [19], which sets the lower bound Δ_s in the constraint.

5) The minimum speed is set to 0 cm/s, which ensures that the patient table does not go back, a standard practice. This sets the upper bound Δ_b.

To identify the coefficients in Eq. (7), observed bolus densities at time t_{k-2}, t_{k-1}, and t_k at position z_k, $z_k + \delta_z$, respectively, are used. The coefficients are obtained in the least squares sense:

$$\hat{a}_i = \arg\min_{a_i} \sum_{\substack{z = z_k, z_k \pm \delta_z \\ t = \bar{t}_k, \bar{t}_{k-1}, \bar{t}_{k-2}}} \left[C(z,t) - \hat{C}(z,t)\right]^2, \tag{12}$$

where $\hat{C}(z,t)$ is given in Eq. (7).

Figure 4 shows the control flow chart of the adaptive bolus chasing CTA.

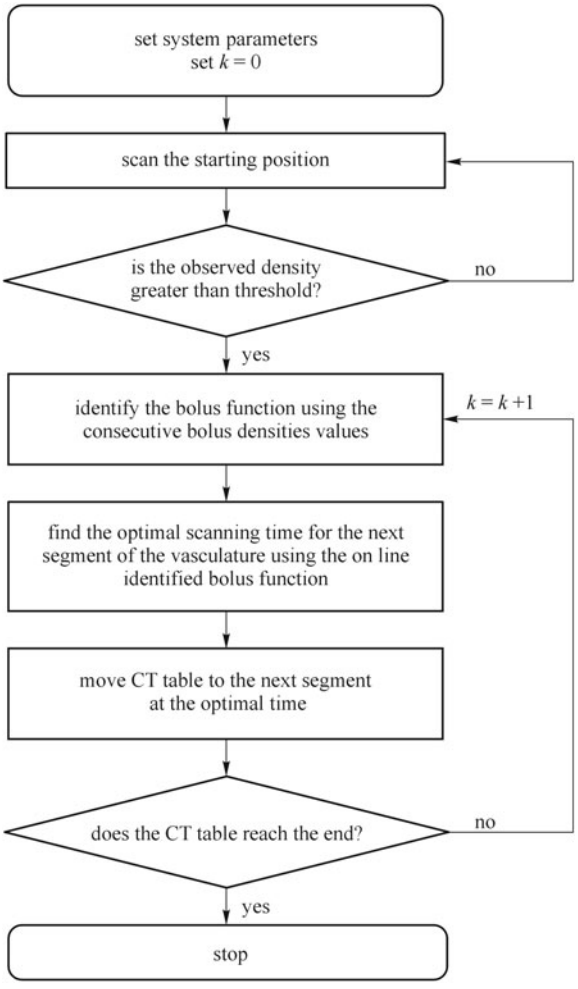

Fig. 4 Control flow chart of adaptive bolus chasing CTA

4 Simulation results

The proposed control algorithm has been tested on the clinical angiogram data. To show the advantage, comparisons were made against the constant-speed method, which is a common practice in clinics. The constant speed is set to 3 cm/s [19]. In all the adaptive control algorithm tests, the upper and lower bounds, Δ_b and Δ_s, are set so the minimum and maximum table speeds correspond to 0 cm/s and 10 cm/s, respectively. The segment, z_e/N, is set to be 5 mm.

The performance indices (PIs) of the adaptive and constant-speed method are compared. They are defined as the ratio of the summation of the scanned density and the summation of the maximum possible density at each segment:

$$\begin{aligned} I_a &= \frac{\sum C(z_k, \bar{t}_k)}{\sum C(z_k, t_k^*(z_k))}, \\ I_c &= \frac{\sum C(z_k, cz_k + t_0)}{\sum C(z_k, t_k^*(z_k))}, \end{aligned} \tag{13}$$

where c is chosen so that the constant speed is 3 cm, and $\sum C(z_k, t_k^*(z_k))$ is the summation of the maximum

possible bolus density, which may not be achievable due to the constraints.

Simulation results of six patients are shown in Table 1. It shows the tracking performance of the adaptive and constant-speed method on six patients. It can be seen in Table 1 that the average I_a is 11% higher than average I_c. Obviously, the adaptive method outperforms the constant one. Figures 5 and 6 provide the detailed results of two patients. In Fig. 5, the upper plot shows the tracking trajectories of adaptive method (red solid), the constant speed (green dash-dot), and the actual maximum density curve on the bolus time-distance contour, where the inner curve the means the higher density level. Both methods catch the bolus at the beginning, but the constant-speed method missed the bolus after a few seconds. In Fig. 6, the upper plot shows the tracking trajectories of adaptive method (red solid), the constant speed (green dash-dot), and the actual maximum density curve on the bolus time-distance contour, where the inner curve the means the higher density level. The constant-speed method misses the bolus at the beginning and middle, but it catches the bolus at the end of the scan. The adaptive method varies its

Table 1 Performance index of adaptive and constant-speed method for six patients

patient	PI of adaptive method (I_a)	PI of constant method (I_c)
1	0.95	0.84
2	0.89	0.79
3	0.98	0.87
4	0.95	0.91
5	0.94	0.86
6	0.92	0.84
average	0.94	0.85

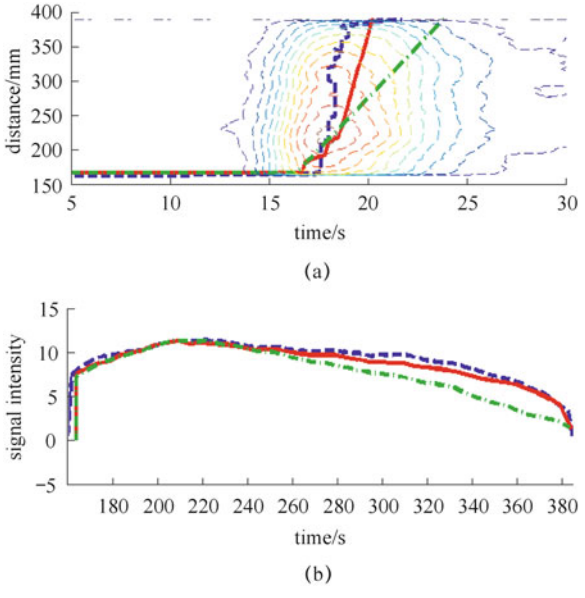

Fig. 5 Tracking results for patient 1

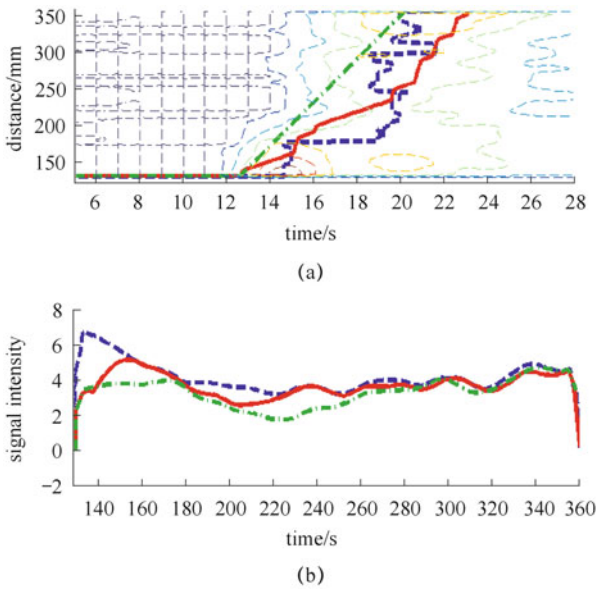

Fig. 6 Tracking results for patient 2

speed, while the bolus maximum position changes. It can be seen from Figs. 5 and 6 that the first patient has a strong heart function, and the contrast bolus flows faster in the aorta. The constant-speed method catches the bolus at the beginning, but it is far behind the bolus peak after a few seconds. On the other hand, the adaptive method is able to track the bolus well for most of the segments. The results of the second patient are more interesting. The constant-speed method over-chases the bolus at the beginning but covers it well at the end of the scan. These two examples demonstrate that the constant-speed method relies largely on luck due to the unknown bolus dynamics. In contrast, the adaptive method ensures an optimal scan regardless of the bolus dynamics.

Remark For the constant-speed method, the optimal starting time (threshold) and constant speed value is unknown a priori. Those choices are purely based on experience. In the above simulations, the starting time and constant speed are good choices, though its performance is still not as good as the adaptive method.

One reason that the constant-speed method results are not too bad is that we only track the contrast bolus in the aorta portion. In this area, the contrast bolus movement is relatively constant. For a long scan length, however, the advantage of the adaptive method becomes more apparent.

5 Experimental results

The proposed adaptive bolus chasing techniques were tested. Figure 7 is a photo of the experimental setup. The pump system, the plastic tube filled with water, and reservoirs are all placed on the CT table and used to

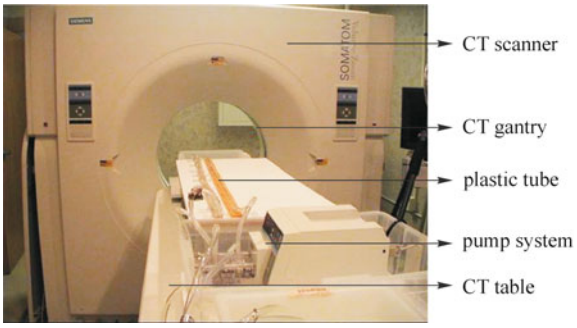

Fig. 7 Experimental setup

simulate the blood system. When the pump is turned on, it drives the bolus inside the tube. The bolus velocity can be changed by varying the pump speed. During the scan, the bolus cross-sectional image is shown on the monitor by real-time image reconstruction algorithms. A frame grabber is used to capture the CT images and feed the bolus information into the controller. The controller predicts the bolus peak position at the next sampling time and sends a command to move the table accordingly. Thus, the bolus peak is kept directly under the CT imaging aperture.

5.1 Experimental setup

1) Phantom and contrast material

A vasculature phantom was designed and built for the bolus chasing experiment (Fig. 8). The phantom has the same geometry as that of a normal male adult. An actual contrast agent mixed with a red dye was used as the contrast bolus, and it was driven by a programmable pump.

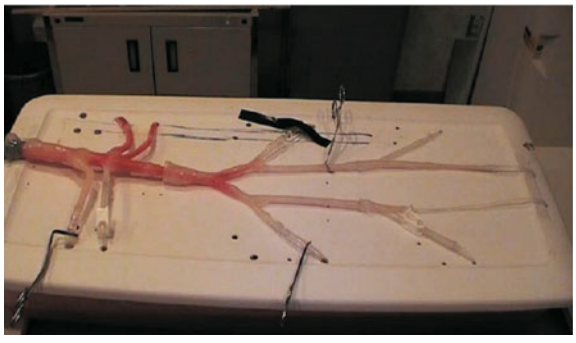

Fig. 8 Vasculature phantom in bolus chasing experiment

2) CT scanner

CT scanner is a Siemens Somatom Volume Zoom four-slice CT scanner, as shown in Fig. 7, with software version A40A. Siemens has also provided us with the CANbus access and command format in order to control the CT table.

3) Frame grabber

Although we have the CT reconstruction algorithm for varying pitch, we are not able to reconstruct the CT images due to the unavailability of the proprietary raw data. To that end, we split the CT video graphics adapter (VGA) signal, feed it to the controller, and capture it using a frame grabber. The frame grabber, manufactured by the NCast Corporation (http://www.ncast.com/DigiCaptureCard.html), is a Digitizer 3.0 Capture Card. It supports standard VGA input modes with a frequency of up to 85 Hz and a maximum resolution of 1280×1024, and is able to capture the image signal at a speed of 30 fps.

4) Pump system

The blood vascular system is physically simulated by a programmable MasterFlex pump system (HV-07523-60 L/S Brushless Digital Drives, made by the Cole Parmer Company, http://www.masterflex.com) connected to a plastic tube filled with water. By changing the pump head size and speed, the water flow rate can be varied between 0.6 and 3400 mL/min. During the experiment, we adjust the pump speed to achieve the desirable bolus dynamics.

5.2 Experimental results

During the scan, the bolus cross-sectional image, together with the vasculature, was shown on the monitor by real-time image reconstruction algorithms. A frame grabber captured the CT images and fed the bolus density information to the controller. The controller determined the optimal scan time for the next position and sent a command to move the CT table accordingly. Due to the proprietary issues, we were unable to completely fulfill our control scheme. First, the real-time raw data was not available, which restrained us from using the actual bolus density information. Second, CT table control was through the CANbus line, which caused control delay [20]. To that end, we had to scale down the flow rate, especially in the part of the aorta. However, the flow rate in the lower limbs changed very little according to our measurement.

Figure 9 shows the tracking results for the adaptive

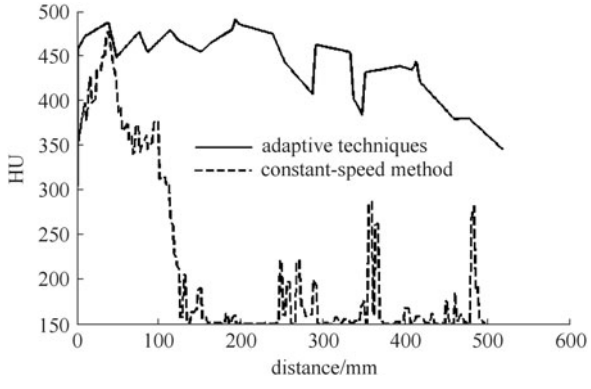

Fig. 9 Scanned bolus density for adaptive techniques (solid) and constant-speed method (dashed)

method and the constant-speed for a 500-mm long artery phantom (starting at the aorta). The constant-speed method was set as 3 cm/s. For all the segments along the artery, the obtained bolus CT number, denoted by housefield unit (HU), of the adaptive method is above 350 HU except for some portion of the end; while the constant-speed method only catches the bolus near the beginning to roughly 100 mm and misses the bolus for the rest 400 mm. This is caused by over-chasing, which is a common occurrence in the clinics.

Remark 1) During the scan, the CT display center is set at 400 and window 250. The HU value of the bolus is transformed into pixel value between 0 and 255. The final HU is transformed back from pixel value on the screen. Therefore, 150 HU actually means a very low density, and 650 HU is very high.

2) The HU curve of the adaptive method looks segmented. This is because the adaptive chasing method covers a large distance each time due to the control delay, while the constant-speed method moves the CT table continuously.

3) It is likely that one constant speed produces a relatively good result. However, this only happens when the preset speed value matches the bolus movement, which is generally unknown a priori. On the other hand, there is no need to set a speed value for adaptive method, and the tracking results are ensured to be good.

6 Discussion and conclusions

To track the contrast bolus peak adaptively, we need to vary the CT table speed during the scan and thus vary the pitch, defined as table movement per rotation/slice collimation. To that end, a reconstruction algorithm for variable pitch is requested. Such algorithms have already been developed by our team [21]. Therefore, from the CT reconstruction point of view, the vascular images can be reconstructed although the CT table velocity is varying.

Though the tracking methods are similar to that in Ref. [13], it is emphasized that, in this paper, we use a model derived from the diffusion-convection equation to approximate the bolus function by a local linear time and space parameter varying model. One obvious benefit is the simplicity in terms of the number of unknown parameters, control and identification design and implementation, and also impact on the real-time calculation. In summary, we propose an adaptive method to synchronize the bolus peak and X-ray aperture. Simulation and experimental results show that the proposed method outperforms the current existing constant-speed method substantially. The adaptive bolus chasing method will be a promising CT technique for vascular diseases.

Acknowledgements The work was supported partially by NSF ECS-0555394 and NIH/NIBIB EB004287.

References

1. Fleischmann D, Hallett R L, Rubin G D. CT angiography of peripheral arterial disease. Journal of Vascular and Interventional Radiology, 2006, 17(1): 3–26
2. Ofer A, Nitecki S S, Linn S, Epelman M, Fischer D, Karram T, Litmanovich D, Schwartz H, Hoffman A, Engel A. Multidetector CT angiography of peripheral vascular disease: a prospective comparison with intraarterial digital subtraction angiography. American Journal of Roentgenology, 2003, 180(3): 719–724
3. Jakobs T F, Wintersperger B J, Becker C R. MDCT-imaging of peripheral arterial disease. Seminars in Ultrasound, CT, and MRI, 2004, 25(2): 145–155
4. Brink J A. Contrast optimization and scan timing for single and multidetector-row computed tomography. Journal of Computer Assisted Tomography, 2003, 27(Suppl 1): S3–S8
5. Duddalwar V A. Multislice CT angiography: a practical guide to CT angiography in vascular imaging and intervention. The British Journal of Radiology, 2004, 77(suppl_1): S27–S38
6. Laswed T, Rizzo E, Guntern D, Doenz F, Denys A, Schnyder P, Qanadli S D. Assessment of occlusive arterial disease of abdominal aorta and lower extremities arteries: value of multidetector CT angiography using an adaptive acquisition method. European Radiology, 2008, 18(2): 263–272
7. Wu Z, Qian J. Real-time tracking of contrast bolus propagation in X-ray peripheral angiography. In: Proceedings of IEEE Workshop on Biomedical Image Analysis. 1998, 164–171
8. Aoki S, Nanbu A, Araki T, Shimazu N, Ichikawa T, Kumagai H, Kachi K, Araki T. Active MR tracking system at 0.2T MR, a preliminary report: real time position tracking on interventional MR. Nippon Igaku Hoshasen Gakkai Zasshi, 1997, 57(13): 877–879
9. Czum J M, Ho V B, Hood M N, Foo T K M, Choyke P L. Bolus-chase peripheral 3D MRA using a dual-rate contrast media injection. Journal of Magnetic Resonance Imaging, 2000, 12(5): 769–775
10. Hood M N, Ho V B, Foo T K, Marcos H B, Hess S L, Choyke P L. High-resolution gadolinium-enhanced 3D MRA of the infrapopliteal arteries: lessons for improving bolus-chase peripheral MRA. Magnetic Resonance Imaging, 2002, 20(7): 543–549
11. Kruger D G, Riederer S J, Polzin J A, Madhuranthakam A J, Hu H H, Glockner J F. Dual-velocity continuously moving table acquisition for contrast-enhanced peripheral magnetic resonance angiography. Magnetic Resonance in Medicine, 2005, 53(1): 110–117
12. Steffens J C, Schäfer F K W, Oberscheid B, Link J, Jahnke T, Heller M, Brossmann J. Bolus-chasing contrast-enhanced 3D MRA of the lower extremity: comparison with intraarterial DSA. Acta Radiologica, 2003, 44(2): 185–192
13. Bai E W, Cai Z J, McCabe R, Wang G. An adaptive optimal control design for a bolus chasing computed tomography Angiography. IEEE Transactions on Control Systems Technology, 2008, 16(1): 60–69
14. Blomley M J, Dawson P. Bolus dynamics: theoretical and experimental aspects. The British Journal of Radiology, 1997, 70 (832): 351–359
15. Bassingthwaighte J B, Ackerman F H, Wood E H. Applications of

the lagged normal density curve as a model for arterial dilution curves. Circulation Research, 1966, 18(4): 398–415

16. Wang G, Raymond G M, Li Y, Schweiger G D, Sharafuddin M, Stolpen A H, Yang S, Li Z, Bassingthwaighte J B, Vannier M W. A model of intravenous bolus propagation for optimization of contrast enhancement. Proceedings of SPIE, 2000, 3978: 436–447
17. Harpen M D, Lecklitner M L. Derivation of gamma variate indicator dilution function from simple convective dispersion model of blood flow. Medical Physics, 1984, 11(5): 690–692
18. Cai Z, Stolpen A, Sharafuddin M J, McCabe R, Bai H, Potts T, Vannier M, Li D, Bi X, Bennett J, Golzarian J, Sun S, Wang G, Bai E W. Bolus characteristics based on magnetic resonance angiography. BioMedical Engineering Online, 2006, 5: 53
19. Fleischmann D, Hittmair K. Mathematical analysis of arterial enhancement and optimization of bolus geometry for CT angiography using the discrete Fourier transform. Journal of Computer Assisted Tomography, 1999, 23(3): 474–484
20. Cai Z, Erdahl C, Zeng K, Potts T, Sharafuddin M, Saba O, Wang G, Bai E W. Adaptive bolus chasing computed tomography angiography: control scheme and experimental results. Biomedical Signal Processing and Control, 2008, 3(4): 319–326
21. Yu H Y, Ye Y B, Zhao S Y, Wang G. A backprojection-filtration algorithm for nonstandard spiral cone-beam CT with an *n*-PI-window. Physics in Medicine and Biology, 2005, 50(9): 2099–2111